


# Turbo Positioning Using Link Reliability in Wireless Networks

Kyungsu Yun, Ji Kyu Park, Jae Young Ahn, and Jae Kyun Kwon 

**In wireless positioning systems using range measurements non-line-of-sight (NLOS) links cause estimation errors. Several studies have attempted to improve the positioning performance by mitigating these NLOS errors. These studies, however, have focused on the performance of a dataset consisting of three or more links. Therefore, measurement errors induced by links are averaged, and a reliable link is not fully utilized in the dataset. This paper proposes a Link Reliability based on Range Measurement (LRRM) scheme, which specifies the relative reliability of each link using residuals. The link reliability becomes the input to a Link Residual Weighting (LRW) scheme, which is also proposed as a weighted positioning scheme. Moreover, LRRM and LRW constitute new turbo positioning, where the estimation errors are reduced considerably by iterative updates.**

**Keywords:** Link reliability, LOS detection, TOA, Turbo positioning, Wireless location.

## I. Introduction

Wireless location technology and its related applications has received attention since the development and implementation of the E-911 system [1]. A range of location-based services (LBS) have been studied and applied to real-world problems. LBS requires a highly accurate location estimation of the terminals to ensure service quality [2]. Generally, wireless positioning by radiolocation obtains the distance information between a base station (BS) and a mobile station (MS) by using the time of arrival (TOA) [3], [4], time difference of arrival (TDOA) [5], [6], angle of arrival (AO vA) [7], [8], received signal strength (RSS) [9], [10], or a hybrid scheme [11]. These schemes operate adequately when the signal is conveyed on a line-of-sight (LOS) path, but non-line-of-sight (NLOS) links are quite common in wireless networks and result in erroneous estimations [12]. Many schemes have been studied to reduce the NLOS errors [12]–[14]. An NLOS path usually estimates a longer distance than the actual distance [15]. In a measurement dataset consisting of three or more BS-MS links with the same number of BSs and an MS, an NLOS error increases the candidate area of the MS position in trilateration or triangulation. In other words, if the candidate area is small, the NLOS error will equally be small. This has been utilized to reduce the NLOS errors and improve the positioning accuracy [16]–[22]. However, these approaches do not separate the links in a dataset, and the errors are averaged within the dataset.

Although a location estimation is performed for a dataset with three or more links, attempts are practically made to obtain the reliability for each link. These reliabilities act as weights in a weighted location estimation. The derivation of the link reliability and weighted estimation are repeated iteratively to reduce the estimation errors. Figure 1 shows the block diagram of the proposed turbo positioning

---

Manuscript received Mar. 8, 2017; revised Sept. 2, 2017; accepted Nov. 8, 2017.  
Kyungsu Yun (kadbonow@kiapi.or.kr) is with the Strategic & Planning Division, Korea Intelligent Automotive Parts Promotion Institute, Daegu, Rep. of Korea.

Ji Kyu Park (ther20002@naver.com) and Jae Kyun Kwon (corresponding author, jack@yumail.ac.kr) are with the Department of Electronic Engineering, Yeungnam University, Gyeongsan, Rep. of Korea.

Jae Young Ahn (jyahn@etri.re.kr) is with the Broadcasting and Media Research Laboratory, ETRI, Daejeon, Rep. of Korea.

This is an Open Access article distributed under the term of Korea Open Government License (KOGIL) Type 4: Source Indication + Commercial Use Prohibition + Change Prohibition (<http://www.kogil.or.kr/info/licenseTypeEn.do>).

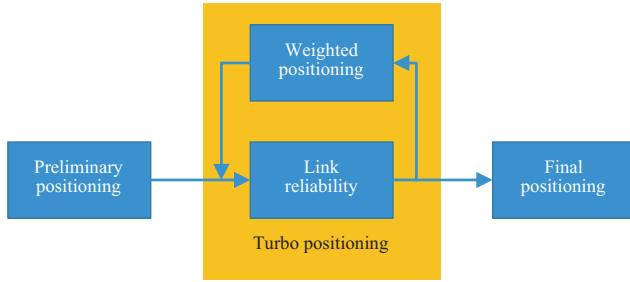


Fig. 1. Concept of turbo positioning.

technique. First, preliminary positioning is used to estimate the initial location of an MS, and any scheme can be applied in this step. Next, the link reliabilities are obtained from the estimated location and range measurements. These reliabilities become weights for the weighted positioning, which produces new estimated locations. Then, the link reliabilities are calculated again, and weighted positioning is performed iteratively. Finally, after a sufficient set of iterations, the final positioning generates an estimate of the MS location. The proposed turbo positioning is characterized by three advantages:

- The reliability is obtained not for a set of links but rather for an individual BS-MS link.
- The link reliabilities act as weights for weighted positioning.
- The iterative turbo principle offers a significant reduction in the estimation error at the expense of a small increase in complexity.

The next section explains the proposed turbo positioning principle. The simulation environments and comparison results are described in Section III, and conclusions are given in Section IV.

## II. Turbo Positioning

As shown in Fig. 1, the link reliability calculation and weighted positioning are required for turbo positioning. This paper proposes a Link Reliability based on Range Measurement (LRRM) scheme for obtaining the BS-MS link reliability, and a Link Residual Weighting (LRW) scheme for weighted positioning. Turbo positioning is applied based on two components and the required operating conditions are given in this section.

### 1. Link Reliability Based on Range Measurement (LRRM) Scheme

In wireless positioning systems, using good links or assigning higher weightings to the best of the links is better than their collective application without any

discrimination. Therefore, reliable links are utilized preferably to reduce the NLOS errors. This paper proposes an LRRM scheme to obtain the link reliability using the position estimate error derived from the range measurements. Generally, a positioning error arises mainly due to two factors: The first is the measurement error, usually considered as additive, such as a synchronization error or timing error by the measuring equipment. The other originates from multipath and NLOS. As a result, range measurements are modeled as [23]:

$$r = d_{\text{LOS}} + d_{\text{noise}} + d_{\text{NLOS}}, \quad (1)$$

where  $r$  is the estimated distance between BS and MS,  $d_{\text{LOS}}$  is the real distance,  $d_{\text{noise}}$  is the measuring error, and  $d_{\text{NLOS}}$  is the NLOS component. A two-dimensional least-square (LS) estimation with at least three link measurements is given as follows [12]:

$$\hat{x} = \arg \min_x \sum_{i \in S} (r_i - \|x - X_i\|)^2, \quad (2)$$

where  $S$  is the index set of BSs,  $r_i$  is the range measurements between the MS and the  $i$ -th BS,  $x$  is the position of the MS,  $\hat{x}$  is the estimate of the MS position, and  $X_i$  is the position of the  $i$ -th BS. In (2),  $(r_i - \|x - X_i\|)$  is called the  $i$ -th residual of  $x$ . If the dataset of range measurements contains NLOS range measurements, the estimated residuals increase. Therefore, large residuals indicate low reliability due to the NLOS links. This reliability, however, is not for a link but a set of links.

The proposed LRRM scheme obtains the reliability for each link from the residuals. The intermediate reliability of the  $i$ -th link in a set  $S$  can be obtained as follows:

$$R_i(\hat{x}, S) = f_r(r_i, \|\hat{x} - X_i\|), i \in S, \quad (3)$$

where  $f_r(\cdot)$  is the function transforming a measurement or a residual to an intermediate reliability. The absolute value of the residual  $f_r(\cdot)$ , is used in this paper:

$$R_i(\hat{x}, S) = |r_i - \|\hat{x} - X_i\||, i \in S. \quad (4)$$

The number of range measurements (BSs) is assumed to be  $M (> 3)$ . Hence, there are  $N = \sum_{i=3}^M \binom{M}{i}$  possible combinations for positioning, and each combination set of BSs and the corresponding estimated position are  $S_k$  and  $\hat{x}_k$ , respectively. For example, when the number of BSs,  $M$  is 5, wireless locations are possible for three BSs, four BSs, or five BSs. There are 10 subsets with three elements out of five members, five subsets with four elements, and a subset with all five elements. Therefore, 16 subsets are eligible for wireless locations, and they are named from  $S_1$

to  $S_{16}$ . For each  $S_k$ ,  $\hat{x}_k$  is the position estimate derived only from BSs in  $S_k$ . For the  $i$ -th link, several intermediate reliability values ( $R_{ik}$ 's) are found in the sets ( $S_k$ 's) containing  $i$ . These intermediate reliability values are processed to the link reliability of the  $i$ -th link,  $\tilde{R}_i$  by the function  $f_R(\cdot)$ .

$$R_{ik}(\hat{x}_k, S_k) = f_r(r_i, \|\hat{x}_k - X_i\|), i \in S_k, \quad (5)$$

$$\tilde{R}_i = f_R(R_{ik}(\hat{x}_k, S_k) | i \in S_k). \quad (6)$$

The process for obtaining the link reliability  $\tilde{R}_i$ , is explained with an example in Table 1. The numbers of BSs and subsets  $S_k$  is 5 and 16, respectively. Each  $S_k$  generates the position estimate  $\hat{x}_k$ , and the intermediate reliability values  $R_{ik}$ 's, are derived for each BS or link in a row-wise manner in the table. Two intermediate reliabilities,  $R_{41}$  and  $R_{51}$  are missing because only BS#1, BS#2, and BS#3 are included in  $S_1$ . For BS#1 or link#1, the derived  $R_{1k}$ 's are processed to one link reliability  $\tilde{R}_1$  in a column-wise manner.

The minimum, average, geometric mean, or weighted average can be used for  $f_R(\cdot)$ . In the case that a weighted average is used, a larger weight is assigned to a good combination set containing an intermediate reliability ( $i \in S_k$ ). In [12], the indicator  $\tilde{R}_{es}$  used to identify good sets is the average of the squared residuals:

$$R_{es}(\hat{x}, S) = \sum_{i \in S} [r_i - \|\hat{x} - X_i\|]^2, \quad (7)$$

$$\tilde{R}_{es}(\hat{x}_k, S_k) = \frac{R_{es}(\hat{x}_k, S_k)}{\text{size of } S_k} = \frac{\sum_{i \in S_k} [r_i - \|\hat{x}_k - X_i\|]^2}{\text{size of } S_k}. \quad (8)$$

A small  $\tilde{R}_{es}(\hat{x}_k, S_k)$  implies a higher reliability set  $S_k$ , and then that the links in  $S_k$  might likely have higher

reliability values. Therefore, the link reliability  $\tilde{R}_i$  in (6) is calculated as follows with the weight of  $(\tilde{R}_{es}(\hat{x}_k, S_k))^{-1}$ .

$$\tilde{R}_i = \frac{\sum_k R_{ik}(\hat{x}_k, S_k) (\tilde{R}_{es}(\hat{x}_k, S_k))^{-1}}{\sum_k (\tilde{R}_{es}(\hat{x}_k, S_k))^{-1}}, i \in S_k. \quad (9)$$

## 2. Link Residual Weighting Scheme

The LRW algorithm updates the estimates of the MS location using the link weights or link reliabilities obtained through the LRRM configuration. The update is performed using weighted averaging, where the link reliabilities work as weights. The conventional weighted positioning schemes position the weight only on a subset of links or the combined data for more than one link, which is in a particular subset, and the relative weights of the links remain unvaried. An estimated MS position for each link is needed to separate the links in the subset. An angle or directional information with a distance estimate for each link is sufficient for this purpose. However, the accurate angle or direction is difficult to obtain.

Figure 2 illustrates the updating procedure for the location estimate. The aim of the entire process is to update the previous position estimate,  $\hat{x}_p$  to  $\hat{x}_w$ . First, the position estimate for link  $i$ ,  $\hat{x}_{Ri}$  is derived. The distance between BS<sub>*i*</sub> and  $\hat{x}_p$  is generally different from the distance estimate  $r_i$ . To update  $\hat{x}_p$  relative to BS<sub>*i*</sub>, a new  $\hat{x}_{Ri}$  is located in the same direction from BS<sub>*i*</sub> with  $\hat{x}_p$ , and the distance between

Table 1. Process from position estimate to link reliability.

| Link or BS index | 1             | 2             | 3             | 4             | 5             |          |
|------------------|---------------|---------------|---------------|---------------|---------------|----------|
| Set index        | $S_1$         | $R_{11}$      | $R_{21}$      | $R_{31}$      |               |          |
|                  | $S_2$         | $R_{12}$      | $R_{22}$      |               | $R_{42}$      |          |
|                  | $S_3$         | $R_{13}$      | $R_{23}$      |               |               | $R_{53}$ |
|                  | $S_4$         | $R_{14}$      |               | $R_{34}$      | $R_{44}$      |          |
|                  | $S_5$         | $R_{15}$      |               | $R_{35}$      |               | $R_{55}$ |
|                  | ...           | ...           | ...           | ...           | ...           | ...      |
| $S_{16}$         | $R_{1,16}$    | $R_{2,16}$    | $R_{3,16}$    | $R_{4,16}$    | $R_{5,16}$    |          |
| Link reliability | $\tilde{R}_1$ | $\tilde{R}_2$ | $\tilde{R}_3$ | $\tilde{R}_4$ | $\tilde{R}_5$ |          |

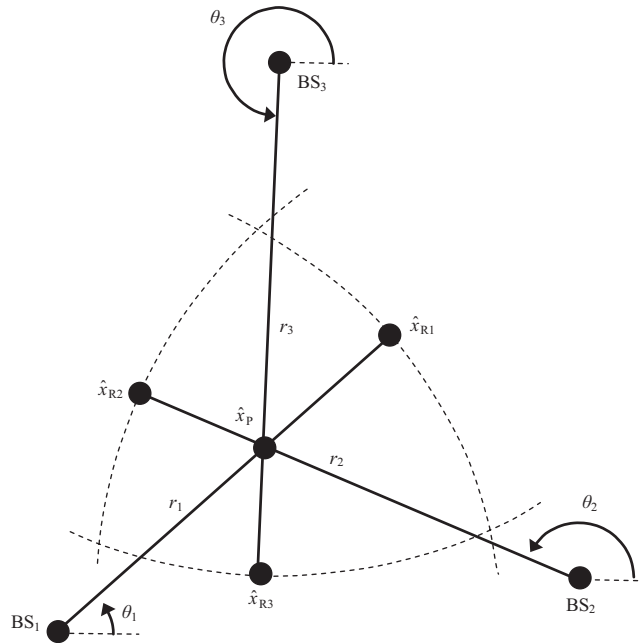


Fig. 2. LRW algorithm.

BS<sub>*i*</sub> and  $\hat{x}_{R_i}$  is set to  $r_i$ . Next, multiple  $\hat{x}_{R_i}$ 's are merged into one new position estimate  $\hat{x}_w$ , which is a weighed position estimate. The previously obtained link reliabilities  $\tilde{R}_i$ 's work as weights  $w_i$ 's, where  $w_i = \tilde{R}_i^{-1}$ . This LRW scheme provides the weighted position estimate,  $\hat{x}_w$  as

$$\hat{x}_w = \frac{\sum_{i \in S} \hat{x}_{R_i} w_i}{\sum_{i \in S} w_i}, \quad (10)$$

where  $\hat{x}_{R_i}$  and  $\hat{x}_w$  are subset-dependent, and  $w_i$  is subset independent. The position estimate for  $S_k$  is called  $\hat{x}_{wk}$ , which becomes the input  $\hat{x}_k$  in a turbo process.

### 3. Turbo Positioning

In the previous subsections, the link reliability is obtained for every single link, and weighted positioning is performed using the link reliabilities. For the former, LRRM is used in (5) and (6), and LRW functions by using (10) for the latter. For the full process depicted in Fig. 1, a positioning scheme yields a preliminary positioning result. In the LRRM scheme, to acquire the link reliabilities, the absolute values of the residuals are used in this study, as shown in (4), to obtain the intermediate reliabilities  $R_{ik}(\hat{x}_k, S_k)$ 's, and (9) computes the link reliabilities  $\tilde{R}_i$  from the intermediate reliabilities. These link reliabilities are passed to the weighted positioning (LRW) phase using  $w_i = f_w(\tilde{R}_i)$ , where  $f_w(\cdot)$  is a function for obtaining the weight from a link reliability. In this paper, a simple inverse was used, that is,  $w_i = \tilde{R}_i^{-1}$ . Equation (10) becomes  $\hat{x}_k$  in (5) for the next turbo iteration. Two further points need to be considered; the final positioning scheme after the turbo iterations should be determined, and the balanced updates of the link reliabilities among the subsets should be guaranteed in the turbo iterations.

Three examples are given for the final positioning. The first scheme is to select three range measurements with the three best link reliabilities, and apply them to trilateration, such as an LS estimation. The second is to apply the residual weighting (Rwgh) [12] scheme as follows, using  $\hat{x}_{wk}$  for  $S_k$  in (10) and  $\tilde{R}_{es}(\hat{x}_{wk}, S_k)$  in (8):

$$\hat{x} = \frac{\sum_{k=1}^N \hat{x}_{wk} (\tilde{R}_{es}(\hat{x}_{wk}, S_k))^{-1}}{\sum_{k=1}^N (\tilde{R}_{es}(\hat{x}_{wk}, S_k))^{-1}}. \quad (11)$$

The third and final scheme is to apply (10) to only the universal set  $S_N (= \{1, 2, 3, \dots, M\})$  for the final positioning. Turbo iterations are performed for all subsets,

and the final positioning is performed only for the universal set. For the final positioning,  $\hat{x}_p$  should be unique in Fig. 2 for (10). Two examples of  $\hat{x}_p$  are to use  $\hat{x}_N$ , the result of the universal set  $S_N$ , and to use the result of the subset where the sum of the reliabilities is best (that is, the smallest). In this paper, we opted for  $\hat{x}_N$ .

The link reliabilities of the subsets should be updated in a balanced way during the turbo iterations. Within a specific subset, an iteration updates the relative superiority of the reliability among links. However, it is difficult to guarantee a balanced update of reliabilities among the subsets. For example, without a balanced update scheme, an inferior LOS link in a good subset might have poorer reliability than a superior NLOS link in a bad subset, despite the LOS link being ideally expected to have a better reliability than the NLOS link. Therefore, a proper scheme, such as the weights for the subsets, is needed. To avoid designing such update scheme, this study uses only the universal set  $S_N$  in the turbo iterations with LRRM and LRW. In particular, turbo iterations and the final positioning are performed only for the universal set except that the preliminary positioning can use any existing scheme, such as LS or Rwgh [12]. Such a simple choice guarantees the stability of the link reliability update and low computational complexity, and also show excellent performances in Subsection III-2.

In summary, this study uses the following simulation scenario for turbo positioning. Since only the universal set  $S_N$  is used, the intermediate reliability is obtained from (3) as:

$$R_i(\hat{x}_p, S_N) = |r_i - \|\hat{x}_p - X_i||, i \in S_N. \quad (12)$$

Equations (6)–(9) are simplified to  $\tilde{R}_i = R_i(\hat{x}_p, S_N)$ , because the  $i$ -th link has only one intermediate reliability. The weight for a link is assumed to be the inverse of the link reliability,  $w_i = f_w(\tilde{R}_i) = \tilde{R}_i^{-1}$ . For turbo feedback,  $\hat{x}_w$  in (13) becomes  $\hat{x}_p$ .

$$\hat{x}_w = \frac{\sum_{i \in S_N} \hat{x}_{R_i} w_i}{\sum_{i \in S_N} w_i}. \quad (13)$$

## III. Performance Evaluation

### 1. Simulation Environments

The performance of the proposed turbo positioning technique was evaluated in a simulation environment. Table 2 lists the simulation parameters based on the 3rd Generation Partnership Project (3GPP) Long Term Evolution (LTE) system. The LTE system provides a sampling interval of 32.552 ns calculated by the sub-

Table 2. Simulation parameters.

| Parameter                 | Value                                      |
|---------------------------|--|
| Sub-carrier spacing       | 15 kHz                                     |
| IFFT/FFT size             | 2,048                                      |
| Basic time unit ( $T_s$ ) | $1/(15,000 \times 2,048)$<br>$= 32.552$ ns |
| Cell layout               | Hexagonal grid (19 cells)                  |
| Inter-site distance       | 1,732 m                                    |
| Number of MSs             | 10,000                                     |
| Oversampling              | $\times 2$                                 |
| Multipath model           | ITU-R M.1225<br>multipath channel model    |

carrier spacing and Inverse Fast Fourier Transform (IFFT)/Fast Fourier Transform (FFT) size, while the sampling frequency is 30.72 MHz. The cell layout uses 19 hexagonal cells, thus 19 range measurements from 19 BSs are given for positioning. The number of subsets provided by 19 elements is  $524,097 \left( = \sum_{n=3}^{19} \binom{19}{n} \right)$ , which is a relatively large number. To reduce the computational complexity, only subsets with three elements are used, and the new number of subsets is  $969 \left( = \binom{19}{3} \right)$ . An MS is generated randomly within the center cell with two tiers. For a simple evaluation, inter-cell interference and noise are ignored. Low inter-cell interference and low noise are realized by the positioning reference signal (PRS) of 3GPP and the high powered PRS, respectively. The performance is determined by using the cumulative distribution function (cdf) for positioning errors.

The proposed turbo positioning method is compared with three schemes: good algorithm, lower-computational-cost residual weighting (LCC-Rwgh) [24], and inverse estimator weighted average (IEWA) [25] schemes. The good algorithm approach is an imaginary scheme, which applies only LOS range measurements to an LS estimation. The discrimination between the LOS and NLOS is assumed to be perfect, and the range measurements have only measurement errors. LCC-Rwgh is a variation of Rwgh, but with lower computational cost. IEWA uses the inverse of the norm of the sum of the residual vectors as a weight, and shows better results than LCC-Rwgh in compensating for NLOS errors.

A range measurement has a measurement error ( $d_{\text{noise}}$ ) and an NLOS error ( $d_{\text{NLOS}}$ ) as given in (1). For  $d_{\text{NLOS}}$ , Pedestrian Channel B (ped-B) and Vehicular Channel A (veh-A) of the International Telecommunication Union-

Table 3. ITU-R M.1225 multipath channel model.

| Tap | Pedestrian channel B |                    | Vehicular channel A |                    | Doppler spectrum |
|-----|----------------------|--------------------|---------------------|--------------------|------------------|
|     | Relative delay (ns)  | Average power (dB) | Relative delay (ns) | Average power (dB) |                  |
| 1   | 0                    | 0                  | 0                   | 0                  | Classic          |
| 2   | 200                  | -0.9               | 310                 | -1.0               | Classic          |
| 3   | 800                  | -4.9               | 710                 | -9.0               | Classic          |
| 4   | 1,200                | -8.0               | 1,090               | -10.0              | Classic          |
| 5   | 2,300                | -7.8               | 1,730               | -15.0              | Classic          |
| 6   | 3,700                | -23.9              | 2,510               | -20.0              | Classic          |

Radiocommunication (ITU-R) M.1225 multipath channel model in Table 3 are used. A channel model provides one LOS tap and five NLOS delay taps with different delay and powers. Note that the delay spread positively correlates to the distance between the BS and MS, but a fixed delay spread is adopted in this paper according to the ITU-R model. The relative delay parameter in Table 3 is converted to a distance, which is actually an NLOS error. The average power of a tap is the average of the square of the absolute value of a random complex Gaussian channel, which effectively becomes the average of an exponential distribution. A range measurement is obtained from the six delay taps. For the frequently used first tap detection, the relative delay is 0, and no error can be modeled. In such case, a random delay should be given for the first tap arrival, but it is difficult to derive a statistical model, which, apparently, is beyond the scope of this paper. Instead, in this study, the maximum power tap among the six taps is selected for a range measurement. Although the first tap has the maximum average power, one of the other taps can also reach the instantaneous maximum value, because this parameter of a tap is randomly generated with its own average. A simple numerical simulation based on the contents of Table 3 generates the selection probability of each tap. For the measurement error  $d_{\text{noise}}$ , the LTE system with a sampling interval of 32.552 ns has a maximum error of  $\pm 4.8828$  m, and doubled oversampling reduces this error to  $\pm 2.4414$  m. In this paper, the measurement error is the rounding error when the sum of the real distance and NLOS error is divided by the oversampling interval and rounded off.

## 2. Simulation Results

This section provides details on the performance evaluation of the proposed turbo positioning technique



based on a few different configurations. These results are used to establish the most appropriate configuration and the number of iterations of the turbo positioning scheme. The turbo positioning scheme is compared to other existing configurations using cdf for positioning errors. A few configurations of the turbo positioning scheme are also compared in Fig. 3. The “bad (weight) turbo” scheme obtains the link intermediate reliabilities for the subsets and merges them into the link reliability by weighted averaging in (9). The positioning estimation is performed using (11). The “bad (min) turbo” scheme differs from the “bad (weight) turbo” setup in that the minimum intermediate reliability value becomes the link reliability in (6). No balancing scheme among the subsets for the link reliability is considered in the above two schemes. The “medium computational cost (MCC) turbo” scheme adopts the computations for the subsets using (4) and (9) only in the first computation of link reliability. For the remaining iterations, the update of the link reliability is performed only on the universal set using (4) and (10). The “LCC turbo” scheme, however, only uses the universal set, even for the first computation. The number of iterations is set to 30, and ped-B channel model is used. As described in Subsection II-3, two “bad turbo” schemes using the subsets without balancing show inferior performance compared to the other two schemes. Because “MCC turbo” and “LCC turbo” demonstrate similar performances, “LCC turbo” with lower computational cost is chosen as the representative configuration, and used for the remaining part of this paper.

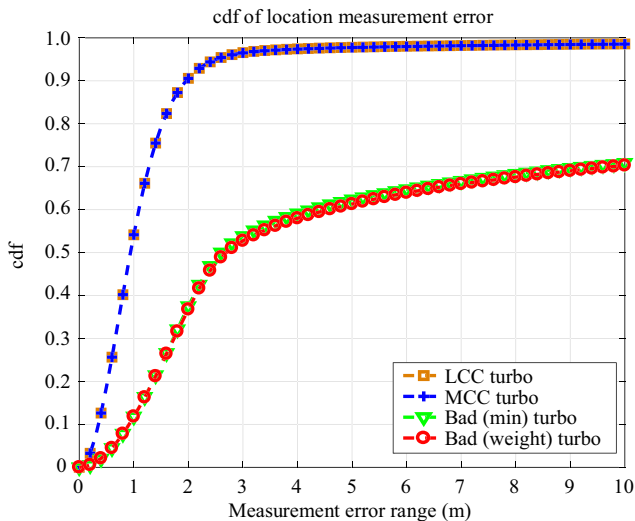


Fig. 3. Performance of the turbo positioning scheme for several configurations.

Figure 4 shows the performance of the turbo positioning scheme based on the number of iterations, up to 50, in the ped-B and veh-A channels. For a more detailed view of the convergence, Fig. 5 expands the results of Fig. 4(a) for an error of 10 m. In other words, the convergence starts at 15 iterations and becomes nearly stationary at 30 iterations.

Figure 6 shows the probability of correctly detecting the LOS links. The number of LOS links within 19 range measurements is assumed to be  $L$ , which is usually equal to or greater than 5. Because a low link reliability indicates a good link, when the link reliabilities are sorted in ascending order, it is best that the  $L$  LOS links appear first. “All LOS BSs” represents the averaged probability of

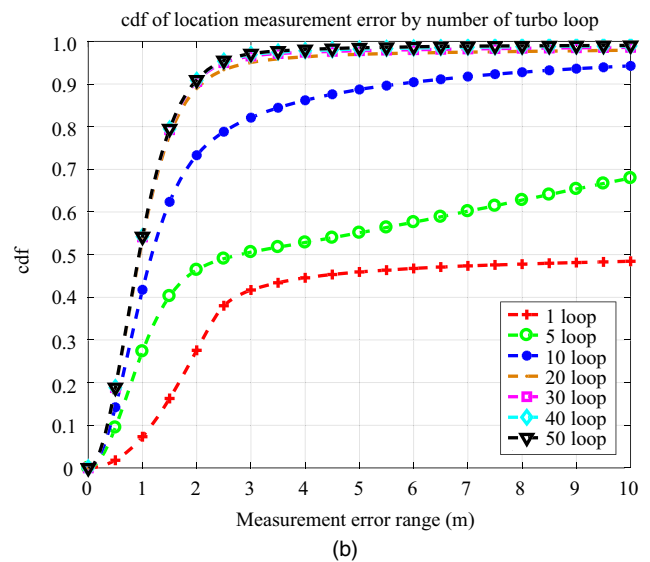
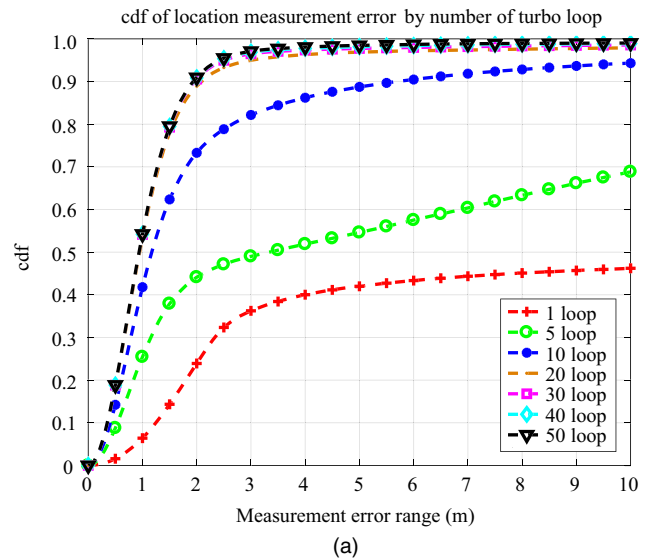


Fig. 4. Performance evaluation based on the number of turbo iterations: (a) ped-B channel and (b) veh-A channel.

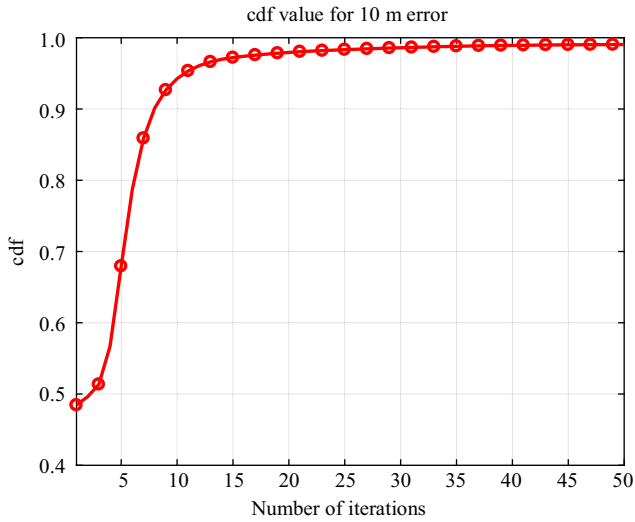


Fig. 5. Probability of a positioning error equal to or less than 10 m based on the number of iterations.

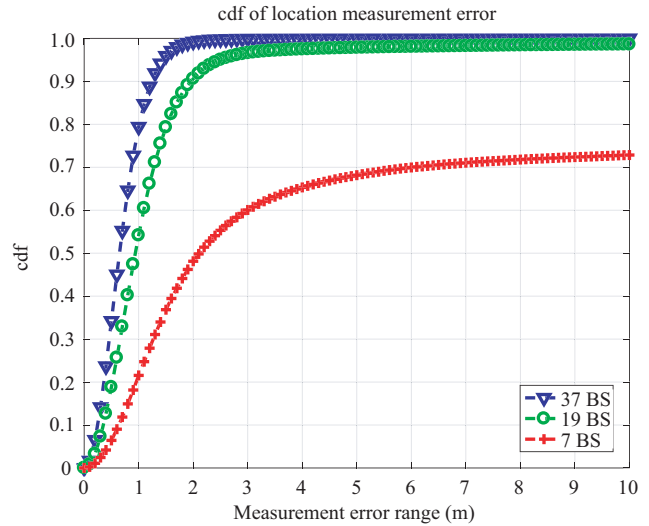


Fig. 7. Performance comparison based on the number of BSs.

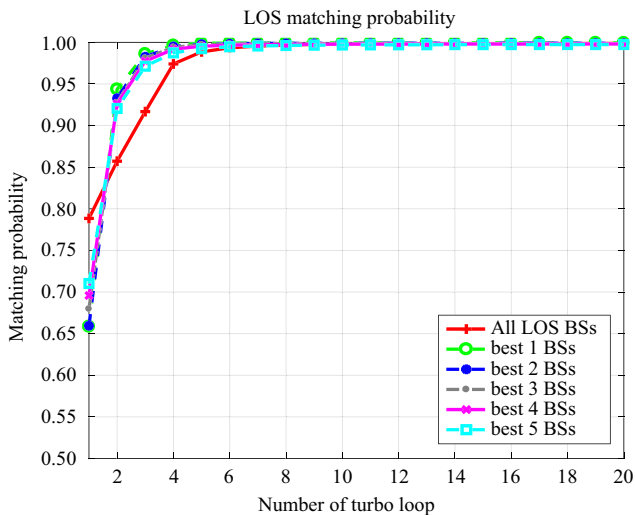


Fig. 6. LOS matching probability based on the number of turbo iterations.

$c/L$ , where the  $c$  links are the LOS type among the first  $L$  links. The “best  $i$  BSs” indicates the averaged probability of  $c = i$ , where  $c$  links are the LOS variety among the first  $i$  set. Because it is essential to find LOS links in trilateration, Fig. 6 can be used to validate the proposed turbo positioning based on the link reliability. In the results, the overall LOS links appear to be detected after eight iterations.

Figure 7 compares the performance of the proposed technique based on the number of BSs. The nominal number of BSs is 19 in this paper, which implies a level up to the second tier. Three values for the number of BSs (7, 19, and 37) are used, and they represent BSs up to the

first tier, the second, and the third, respectively. It is natural that more BSs provide better positioning performance. Results using seven BSs are inferior to the other cases. However, it offers better performance than the “bad turbo” scheme with 19 BSs in Fig. 3, which represents the upper bound among the other schemes seen in Fig. 8. This means that the proposed scheme provides a much better performance with only seven BSs compared to the other options with 19 BSs.

In Fig. 8, the proposed turbo positioning method is compared with the existing schemes. Figure 8(a) shows the measurement errors of up to 1 km, and Fig. 8(b) enhances the plots for errors up to 10 m. In Fig. 8(a), turbo positioning provides a similar performance to the – impractical – good algorithm using only LOS links. This is followed in order by the IEWA and LCC-Rwgh schemes. The LCC-Rwgh scheme shows little contribution to the cdf between a distance of 0.03 km to 0.08 km. The reason for this being that the Rwgh scheme uses the inverse of the sum of the squares of residuals as a weight, and as such, a very large weight value is placed on the best subset. Therefore, performance degradation is inevitable when the best subset contains an NLOS link. Incidentally, the ped-B and veh-A channel models in the simulation provide discrete NLOS errors. Consequently, if the best subset contains only LOS links, the resulting positioning error appears to be less than 0.03 km. Otherwise, the error is rather larger than 0.08 km. However, the IEWA scheme uses the inverse of the norm of the sum of the residual vectors as a weight. A smaller weight than that of the Rwgh scheme results in a smoother rise in the cdf graph. However, such characteristic behavior produces a

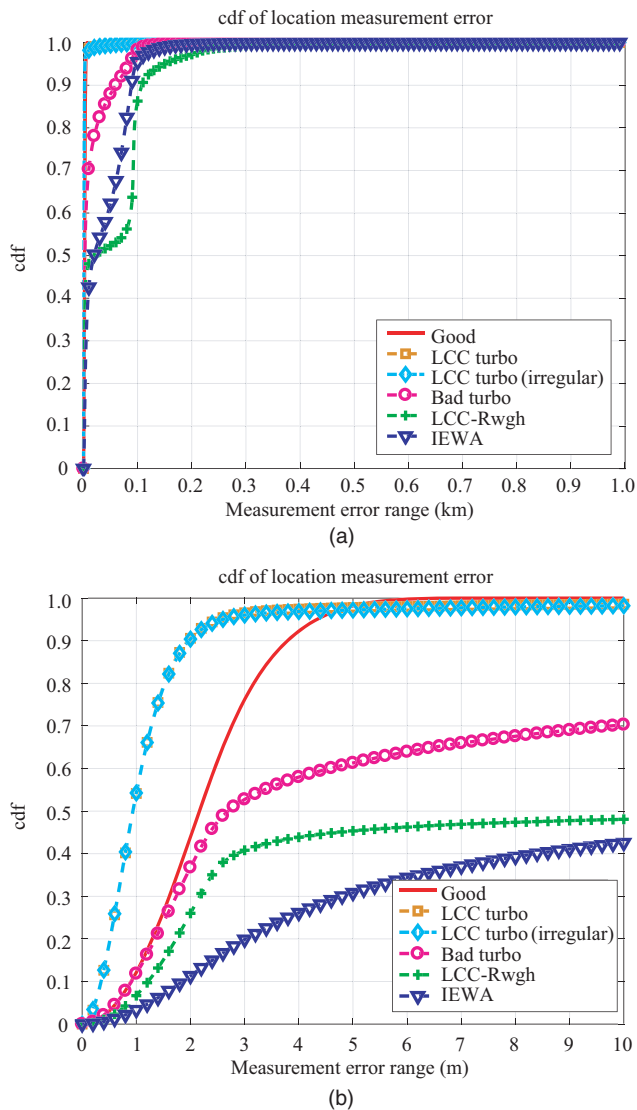


Fig. 8. Performance comparison of the proposed and existing schemes: (a) measurement error range of up to 1 km and (b) measurement error range of up to 10 m.

reversed performance according to the enhanced plots of Fig. 8(b). When the best subset contains only LOS links, the Rwgh scheme places a large weight on the best subset, to ensure that it is superior to the IEWA option. Turbo positioning is shown to definitely reduce NLOS errors in Fig. 8(a). Moreover, the measurement error is compensated for by turbo positioning in Fig. 8(b), where the technique is significantly better than the good algorithm, within an error range of 4 m. However, the superiority is reversed when the error range becomes larger than 4.4 m, mainly because the NLOS errors diminish the performance of the turbo positioning scheme. In addition, the comparison between

regular hexagonal cell deployment and its irregular displacement is also shown in the same figure. BS location is randomly displaced within 100 m, and the case is labeled as “irregular” in the figure. In the comparison to the LCC turbo scheme, performance degradation is shown to be insignificant.

#### IV. Conclusion

This paper has proposed LRRM and LRW schemes for obtaining link reliability as a weight and weighted positioning, respectively. The two schemes were repeated iteratively in the proposed turbo positioning operation. Weighted positioning was shown to provide new position estimates using the link reliabilities as weights, which were, in turn, used to update the link reliabilities. Simulation test results revealed that the performance of the turbo positioning technique was excellent under the stipulated conditions. The number of iterations employed, in the range of 20 to 30 was sufficient for performance convergence. The turbo positioning scheme demonstrated a satisfactory ability in detecting LOS links. Furthermore, its performance was observed to be similar to that of the ideal good algorithm. It is worth noting that the simulation results for turbo positioning were obtained by manipulating only the universal set without significantly considering the balanced updates of the link reliabilities among the subsets.

#### Acknowledgements

This work was supported by the 2015 Yeungnam University Research Grant.

#### References

- [1] J.H. Reed, K.J. Krizman, B.D. Waener, and T.S. Rappaport, “An Overview of the Challenges and Progress in Meeting the E-911 Requirement for Location Service,” *IEEE Commun. Mag.*, vol. 36, no. 4, Apr. 1998, pp. 30–37.
- [2] P. Bellavista, A. Küpper, and S. Helal, “Location-Based Services: Back to the Future,” *IEEE Pervasive Comput.*, vol. 7, no. 2, Apr.–June 2008, pp. 85–89.
- [3] J. Caffery and G.L. Stuber, “Subscriber Location in CDMA Cellular Networks,” *IEEE Trans. Veh. Technol.*, vol. 47, no. 2, May 1998, pp. 406–416.
- [4] J. He, T. Geng, F. liu, and C. Xu, “CC-KF: Enhanced TOA Performance in Multipath and NLOS Indoor Extreme Environment,” *IEEE Sens. J.*, vol. 14, no. 11, Nov. 2014, pp. 3766–3774.



- [5] F. Gustafsson et al., "Particle Filters for Positioning, Navigation, and Tracking," *IEEE Trans. Signal Process.*, vol. 50, no. 2, Feb. 2002, pp. 425–437.
- [6] E. René Játiva, E. Garzón, and J. Vidal, "Space-Time Diversity for NLOS Mitigation in TDOA-Based Positioning Systems," *IEEE Int. Eng. Summit, II Cumbre Int. de las Ingenierias (IE-Summit)*, Boca del Rio, Brazil, Mar. 2–5, 2016, pp. 1–6.
- [7] L. Cong and W. Zhuang, "Hybrid TDOA/AOA Mobile User Location for Wideband CDMA Cellular Systems," *IEEE Trans. Wireless Commun.*, vol. 1, no. 3, July 2002, pp. 439–447.
- [8] P. Gimenez-Febrer, A. Pages-Zamora, S.S. Pereira, and R. Lopez-Valcarce, "Distributed AOA-Based Source Positioning in NLOS with Sensor Networks," *IEEE Int. Conf. Acoust., Speech Signal Process. (ICASSP)*, South Brisbane, Australia, Apr. 19–24, 2015, pp. 3197–3201.
- [9] N. Patwari, A.O. Hero, M. Parkins, N.S. Correal, and R.J. O'Dae, "Relative Location Estimation in Wireless Sensor Networks," *IEEE Trans. Signal Process.*, vol. 51, no. 8, Aug. 2003, pp. 2137–2148.
- [10] R.M. Vaghefi, M.R. Gholami, R.M. Buehrer, and E.G. Strom, "Cooperative Received Signal Strength-Based Sensor Localization with Unknown Transmit Powers," *IEEE Trans. Signal Process.*, vol. 61, no. 6, Mar. 2013, pp. 1389–1403.
- [11] A.H. Sayed, A. Tarighat, and N. Khajehnouri, "Network-Based Wireless Location: Challenges Faced in Developing Techniques for Accurate Wireless Location Information," *IEEE Signal Process. Mag.*, vol. 22, no. 4, July 2005, pp. 24–40.
- [12] P.-C. Chen, "A Non-Line-of-Sight Error Mitigation Algorithm in Location Estimation," *IEEE Wireless Commun. Netw. Conf.*, New Orleans, LA, USA, Sept. 21–24, 1999, pp. 316–320.
- [13] L. Cong and W. Zhuang, "Nonline-of-Sight Error Mitigation in Mobile Location," *IEEE Trans. Wireless Commun.*, vol. 4, no. 2, Mar. 2005, pp. 560–573.
- [14] S. Venkatesh and R.M. Buehrer, "NLOS Mitigation Using Linear Programming in Ultrawideband Location-Aware Networks," *IEEE Trans. Veh. Technol.*, vol. 56, no. 5, Sept. 2007, pp. 3182–3198.
- [15] Y.T. Chan, W. Tsui, H. So, and P. Ching, "Time-of-Arrival Based Localization under NLOS Conditions," *IEEE Trans. Veh. Technol.*, vol. 55, no. 1, Jan. 2006, pp. 17–24.
- [16] W. Wang, Z. Wang, and B. O'Dea, "A TOA-Based Location Algorithm Reducing the Errors due to Non-Line-of-Sight (NLOS) Propagation," *IEEE Trans. Veh. Technol.*, vol. 52, no. 1, Jan. 2003, pp. 112–116.
- [17] S. Mazuelas et al., "Prior NLOS Measurement Correction for Positioning in Cellular Wireless Networks," *IEEE Trans. Veh. Technol.*, vol. 58, no. 5, June 2009, pp. 2585–2591.
- [18] A. Bahillo et al., "Indoor Location Based on IEEE 802.11 Round-Trip Time Measurements with Two-Step NLOS Mitigation," *Prog. Electromag. Res. B*, vol. 15, 2009, pp. 285–306.
- [19] K. Lee, J. Oh, and K. You, "TDOA/AOA Based Geolocation Using Newton Method under NLOS Environment," *IEEE Int. Conf. Cloud Comp. Big Data Anal (ICCCBDA)*, Chengdu, China, July 5–7, 2016, pp. 373–377.
- [20] R.M. Vaghefi, J. Schloemann, and R.M. Buehrer, "NLOS Mitigation in TOA-Based Localization Using Semidefinite Programming," *Workshop Posit. Nav. Commun. (WPNC)*, Dresden, Germany, Mar. 20–21, 2013, pp. 1–6.
- [21] J.M. Pak, C.K. Ahn, P. Shi, Y.S. Shmaliy, and M.T. Lim, "Distributed Hybrid Particle/FIR Filtering for Mitigating NLOS Effects in TOA Based Localization Using Wireless Sensor Networks," *IEEE Trans. Ind. Electron.*, vol. 64, no. 6, June 2017, pp. 5182–5191.
- [22] Y. Lei, M. Wang, and N. Xiao, "NLOS Error Mitigation in Mobile Location Based on TOA Reconstruction," *Inform. Commun. Technol. (IETICT 2013)*, Beijing, China, Apr. 27–29, 2013, pp. 475–480.
- [23] G.-L. Sun and W. Guo, "Bootstrapping M-Estimators for Reducing Errors due to Non-Line-of-Sight (NLOS) Propagation," *IEEE Commun. Lett.*, vol. 8, no. 8, Aug. 2004, pp. 509–510.
- [24] L. Jiao, J. Xing, X. Zhang, J. Zhang, and C. Zhao, "LCC-Rwgh: a NLOS Error Mitigation Algorithm for Localization in Wireless Sensor Network," *IEEE Int. Conf. Control Autom.*, Guangzhou, China, May 30–June 1, 2007, pp. 1354–1359.
- [25] N. Bhagwat and B. Jabbari, "Analysis of Localization Accuracy in Wireless Networks in Presence of Uncertain Beacon Positions," *IEEE Global Telecommu. Conf.*, Miami, FL, USA, Dec. 6–10, 2010, pp. 1–5.



**Kyungsu Yun** received his PhD degree in electronic engineering from Yeungnam University, Gyeongsan, Rep. of Korea, in 2015. Since 2016, he has been a researcher at the Korea Intelligent Automotive Parts Promotion Institute, Daegu, Rep. of Korea. His research interests include autonomous vehicles, deep learning, and wireless positioning.



**Ji Kyu Park** received his BS degree in electronic engineering from Yeungnam University, Gyeongsan, Rep. of Korea, in 2016. He is currently working towards an MS degree in electronic engineering at Yeungnam University. His research interests include visible light communications, underwater communications, and wireless location.



**Jae Young Ahn** received his BS, MS, and PhD degrees in engineering from Yonsei University, Seoul, Rep. of Korea, in 1983, 1985, and 1989, respectively. Since 1989, he has been with the ETRI, Daejeon, Rep. of Korea. From 1989 to 2016, he was involved in the development of satellite communications systems, wireless LAN technologies, and radio transmission schemes for mobile communications in the ETRI. Since 2017, he has been with the Autonomous Unmanned Vehicle Research Division, ETRI, where he is now an assistant vice president. His current research interests include the advanced radio transmission schemes for wireless and mobile communications and the autonomous operation of unmanned vehicles.



**Jae Kyun Kwon** received his BS, MS, and PhD degrees in electrical engineering from Korea Advanced Institute of Science and Technology, Daejeon, Rep. of Korea, in 1996, 1998, and 2003, respectively. From August 2003 to August 2006, he was a senior researcher with the ETRI, Daejeon, Rep. of Korea. Since 2006, he has been with the Department of Electronic Engineering, Yeungnam University, Gyeongsan, Rep. of Korea, where he is now a professor. His research interests include visible light communications, underwater communications, and wireless location.